Rapid Acidification of Endocytic Vesicles Containing Asialoglycoprotein in Cells of a Human Hepatoma Line

BENJAMIN TYCKO, CHARLES H. KEITH, and FREDERICK R. MAXFIELD
Department of Pharmacology, New York University Medical Center, New York 10016

ABSTRACT Acidification of endocytic vesicles has been implicated as a necessary step in various processes including receptor recycling, virus penetration, and the entry of diphtheria toxin into cells. However, there have been few accurate pH measurements in morphologically and biochemically defined endocytic compartments. In this paper, we show that prelysosomal endocytic vesicles in HepG2 human hepatoma cells have an internal pH of approximately 5.4. (We previously reported that similar vesicles in mouse fibroblasts have a pH of 5.0.) The pH values were obtained from the fluorescence excitation profile after internalization of fluorescein labeled asialo-orosomucoid (ASOR). To make fluorescence measurements against the high autofluorescence background, we developed digital image analysis methods for estimating the pH within individual endocytic vesicles or lysosomes. Ultrastructural localization with colloidal gold ASOR demonstrated that the pH measurements were made when ligand was in tubulovesicular structures lacking acid phosphatase activity. Biochemical studies with ^{125}I-ASOR demonstrated that acidification precedes degradation by more than 30 min at 37°C. At 23°C ligand degradation ceases almost entirely, but endocytic vesicle acidification and receptor recycling continue. These results demonstrate that acidification of endocytic vesicles, which causes ligand dissociation, occurs without fusion of endocytic vesicles with lysosomes. Methylamine and monensin raise the pH of endocytic vesicles and cause a ligand-independent loss of receptors. The effects on endocytic vesicle pH are rapidly reversible upon removal of the perturbant, but the effects on cell surface receptors are slowly reversible with methylamine and essentially irreversible with monensin. This suggests that monensin can block receptor recycling at a highly sensitive step beyond the acidification of endocytic vesicles. Taken together with other direct and indirect estimates of endocytic vesicle pH, these studies indicate that endocytic vesicles in many cell types rapidly acidify below pH 5.5, a pH sufficiently acidic to allow receptor-ligand dissociation and the penetration of some toxin chains and enveloped virus nucleocapsids into the cytoplasm.

We recently demonstrated that endocytic vesicles in mouse fibroblasts become acidified shortly after formation (31), and suggested that this early acidification of endocytic vesicles may be a necessary step in processes such as receptor recycling and the penetration of enveloped viruses and diphtheria toxin into the cytoplasm. While there have been several recent studies that support this hypothesis through indirect evidence, there have been very few direct measurements of the pH of endocytic vesicles. In addition to our measurement in mouse fibroblasts using fluorescein-labeled α_2-macroglobulin as a pH probe, van Renswoude et al. (34) have shown that fluorescein-labeled transferrin taken up by erythroleukemic cells is in nonlysomal intracellular compartments with an average pH of 5.5. The morphological identity of the compartments involved in transferrin uptake have not yet been reported. Accurate measurements in other systems have been hampered by high levels of cellular autofluorescence and the reduced intensity of fluorescein fluorescence at acid pH values. In this paper, we describe methods, including digital image analysis, for obtaining accurate pH measurements using fluorescein labeled ligands even in the presence of high levels of cellular autofluorescence. We apply these methods to determine the pH of prelysosomal endocytic vesicles containing fluorescein-labeled asialoorosomucoid (F-ASOR)[1] in HepG2 human hep-

[1] *Abbreviations used in this paper:* ASOR, asialoorosomucoid; F-ASOR, fluorescein-labeled ASOR; FITC, fluorescein isothiocyanate; FITC-dextran, fluoresceinated dextran; αMEM, α-modified Eagle's medium; PBS, phosphate-buffered saline.

THE JOURNAL OF CELL BIOLOGY · VOLUME 97 DECEMBER 1983 1762-1776

atoma cells. This system was chosen for study because the pathways of asialoglycoprotein endocytosis have been extensively studied by biochemical and morphological methods (2, 26, 35, 37).

Desialated glycoproteins bind to hepatocyte surface receptors that aggregate over clathrin coated pits (35). The ligands are internalized into tubulovesicular structures and are ultimately delivered to lysosomes (2, 10, 11, 35), while the receptors recycle to the plasma membrane (26). Morphological and biochemical studies have shown that ligands dissociate from their receptors within the cell in a nonlysosomal compartment (11, 14, 35). Kinetic studies using the HepG2 hepatoma cell line (26) or isolated hepatocytes (6) have led to the development of quantitative analyses for the rates of internalization, ligand degradation, and receptor recycling. When HepG2 cells are incubated with half-saturating concentrations of asialoorosomucoid (ASOR), a receptor completes a cycle of binding, internalization, and return to the surface every 16 min. However, ligand degradation does not begin until ~45 min after endocytosis. Because of the long lag between endocytosis and degradation, the HepG2 cells are an excellent system for studying prelysosomal endocytic vesicles.

In this paper, we demonstrate that endocytic vesicles in HepG2 cells have an internal pH of 5.3–5.5. The pH gradient across the vesicle membrane is dissipated by methylamine or monensin. As recently reported for isolated hepatocytes (14), we find that monensin prevents the intracellular dissociation of ASOR from its receptor in HepG2 cells. Methylamine and monensin both cause a ligand-independent depletion of cell surface receptors. These results support the hypothesis that endocytic vesicle acidification plays a critical role in receptor recycling.

MATERIALS AND METHODS

Reagents: Fluorescein isothiocyanate (FITC), and HEPES were obtained from Research Organics. Monensin (Calbiochem-Behring Corp., San Diego, CA) was dissolved in ethanol at 10 mM and diluted in medium 1 (defined below, see Binding Experiments) at 20 μM before adding it to cells. The $Na^{125}I$ was obtained from New England Nuclear (Boston, MA). All other reagents were obtained from Sigma Chemical Co. (St. Louis, MO) unless otherwise specified. PBS contained sodium chloride (130 mM), potassium chloride (5 mM), and sodium phosphate (20 mM), pH 7.4.

Cell Culture: HepG2 cells were provided by Drs. B. Knowles and D. Aden of the Wistar Institute. The cells were grown in α-modified Eagle's medium (αMEM, Gibco Laboratories) containing 5% fetal bovine serum and 5% horse serum. Cells were grown in a humidified incubator at 37°C under 5% CO_2. Cells were subcultured (Trypsin-EDTA, Gibco Laboratories) at ratios of not less than 1 to 3, and were grown in 35-mm plastic dishes for 4 d before most experiments. For fluorescence microscopy, 35-mm dishes were drilled through the center to form a 10-mm diameter hole. A glass coverslip was affixed to the bottom of the dish, covering the hole, with a small amount of hot paraffin-vaseline (3:1). Dishes with coverslips were then derivatized with polylysine (20 μg/ml in H_2O for 2 h) and sterilized by UV irradiation. Polylysine derivatization was necessary to promote spreading of cells on the glass substratum.

Preparation of F-ASOR: Orosomucoid (50 mg) was dissolved in 1 ml of 50 mM acetate buffer, pH 5, to which was added 0.6 IU of neuraminidase. The solution was left overnight at 37°C, followed by an additional 0.6 IU of neuraminidase for 6 h at 37°C. The removal of sialic acid was complete as measured by the thiobarbituric acid assay (36). Neuraminidase was removed by passing the solution over a 1.5-ml column of oxamic acid-Sepharose essentially as described (7). The ASOR (5 mg in 1 ml of PBS in dialysis tubing) was fluorescein-labeled by dialysis overnight at 4°C against FITC (20 mg in 40 ml of 50 mM borate buffer, pH 9.0), followed by chromatography on Sephadex G25 (column volume 10 ml) to remove free fluorescein. The F-ASOR, stored in PBS at 4°C, retained binding activity for up to one month.

Preparation of ^{125}I-ASOR: ASOR (300 μg in 50 μl of PBS) was added to $Na^{125}I$ (1 mCi in 25 μl of 0.3 M phosphate buffer, pH 7). Iodination was initiated by addition of chloramine T (20 μg in 10 μl of water) and allowed to proceed for 1 min. The reaction was stopped by addition of sodium metabisulfite (40 μg in 10 μl of water). After separation from free iodide by chromatography over Sephadex G25, the ^{125}I-ASOR was >90% precipitable by 10% trichloroacetic acid and had a specific activity between 1.0×10^6 cpm/μg and 8.0×10^6 cpm/μg in various preparations.

Preparation of ASOR Conjugated to Colloidal Gold (ASOR-Gold): Colloidal gold (10–20-nm diameter) was prepared by the ascorbic acid method as described (8) and was titrated with ASOR using stability to flocculation on addition of an equal volume of 10% sodium chloride as the criterion for saturation with protein. The ASOR-gold (50 ml) was pelleted by centrifugation at 20,000 *g* for 35 min and washed twice by resuspension in 5 mM HEPES buffer, pH 7.0, and recentrifugation. The final preparation, obtained by resuspension of the loose pellet in one ml of residual buffer, had an ASOR concentration of 25 μg/ml and was stable for at least 1 wk when stored at 4°C. Addition of polyethylene glycol as a stabilizer was not found to be necessary.

Binding Experiments: The medium used in all binding experiments (medium 1) contained 140 mM sodium chloride, 4 mM potassium chloride, 1.5 mM calcium chloride, 20 mM glucose, 2 mg per ml of bovine serum albumin and 20 mM HEPES buffer, pH 7.4. To measure surface binding, we incubated cells with ^{125}I-ASOR in medium 1 at 37°C for 10 min followed by rinsing and reincubation for the indicated times at the indicated temperatures. In experiments meauring the internalization kinetics of ^{125}I-ASOR, the surface-bound ligand was removed from cells by addition of PBS containing 5 mM EDTA at 23°C for 1 min. Removal of surface-bound ligand was >90% under these conditions. Radioactivity was measured in a Beckman 4000 gamma counter (Beckman Instruments, Palo Alto, CA).

Ligand Dissociation Assay: The procedure of Bridges et al. (6) was used with slight modifications to determine whether intracellular ^{125}I-ASOR was bound to its receptor. After incubation with ^{125}I-ASOR, cells were solubilized in a buffer (0.7 ml/35-mm dish) containing 1% Triton X-100, 10% calf serum, 20 mM $CaCl_2$, and 50 mM Tris-HCl, pH 7.6. Unlabeled ASOR (200 μg/ml) was included in the solubilization buffer to prevent reassociation of dissociated ligand during solubilization. In some experiments calcium was chelated by addition of 40 mM sodium EDTA to the solubilization buffer. After solubilization on ice for 10 min with occasional vortexing, the ligand-receptor complexes were precipitated by addition of an equal volume of ice-cold saturated ammonium sulfate. Free ligand is not precipitated under these conditions. The ligand-receptor complexes were separated from free ligand by filtration of an aliquot of 0.35 ml from each tube through a 0.45-μm pore size Millipore filter that had been prerinsed with solubilization buffer. The precipitate was rinsed with 0.5 ml of ice-cold 60% saturated ammonium sulfate, and the filter-bound radioactivity was counted in parallel with the total radioactivity in each tube.

Fluorescence Microscopy: The microscope was a Leitz Diavert fluoresence microscope with interchangeable narrow band pass filters (E. Leitz, Inc., Rockleigh, NJ). The system for silicon intensification video fluorescence microscopy has been described (31). The microscope is equipped with a photomultiplier tube and measuring diaphragm that allows fluorescence intensity measurements from single cells or groups of cells. To measure the vesicle pH, we incubated cells with F-ASOR on the microscope stage, maintained at 37°C by an air curtain heater as has been described (31). The cellular autofluorescence with excitation at 450 and 490 nm was measured from a group of two or three cells before addition of the F-ASOR and was subtracted as background from the signal obtained from the same field after a 10-min incubation with F-ASOR (100 μg/ml) and a 5-min rinse. The autofluorescence was variable but was as much as 90% of the total signal when the measurements were made from living cells (autofluorescence contributed up to 70% of the total signal from cells that were fixed and exposed to methylamine to dissipate pH gradients). Nevertheless, after correction for autofluorescence the standard errors in the measurements of the ratio of fluorescence intensities with excitation at 450 and 490 nm (the 450/490 ratio) were low (see Table II). Fluorescence images of living cells which had endocytosed F-ASOR were recorded on videotape and digitized as described below. To measure lysosomal pH, cells were incubated with FITC-dextran (40,000 mol wt) at 2 mg/ml in αMEM with 10% fetal bovine serum overnight at 37°C, rinsed with medium 1, and transferred to the microscope stage. Fluorescence images were recorded on videotape and digitized as described below.

Image Digitization and Processing: Video images were obtained using a Dage/MTI 65 MKII SIT camera. The camera was modified by Video Measurements Inc. (Elmsford, NY) to provide complete manual control of gain and black level and to linearize the intensity response curve. Images were recorded on a Panasonic NV8030 video tape recorder with the recorder gain in the manual position. Images were digitized using a CAT-800 Image Digitizer (Digital Graphics, Inc., Palo Alto, CA) housed in a Northstar 64K microcom-

puter. The digitizer divides the image into a 484 × 512 matrix of picture elements ("pixels"). Each pixel is assigned an intensity from 0-255 (8 bits) by a high speed A/D converter. One complete image (256,000 k Bytes) is digitized and stored in the CAT-800 memory in 1/30 s. Digitized images are transmitted to a MINC 11/23 (Digital Equipment Corporation) for processing. Processed images are transmitted back to the CAT-800 for display on a video monitor. Digitized images are stored on Winchester disks.

To improve the signal-to-noise ratio for the digitized images, we averaged the pixel intensities in four to eight video frames before processing. The system was tested using human fibroblast cells that had been incubated with fluorescein-labeled α_2-macroglobulin (150 μg/ml) for 30 min, rinsed and fixed with 2% formaldehyde in PBS. To check the system linearity, we recorded images of cells with the incident illumination attenuated by a series of neutral density filters which covered the range from 6% to 100% of full illumination. The total image intensity and the intensity of individual bright dots in the field were both linear in this range of illumination.

Staining for Acid Phosphatase: Cells were incubated with F-ASOR in medium 1 for 10 min at 37°C followed by a 5-min rinse or with FITC-dextran (2 mg/ml) in αMEM containing 5% fetal bovine serum and 5% horse serum overnight, followed by rinsing in PBS containing 1 mM calcium chloride. Cells were fixed for 30 min in 2% formaldehyde in PBS containing 1 mM calcium chloride. The dishes were rinsed overnight in 140 mM sodium cacodylate buffer, pH 7.3. The substrate for acid phosphatase was β-glycerophosphate (10 mM) in Tris-maleate buffer (50 mM) containing 5% sucrose, pH 4.5. Cells were incubated with substrate at 37°C for 1 h, rinsed in sodium cacodylate buffer (140 mM, pH 7.3), exposed to 0.5% ammonium sulfide for 5 min, rinsed in cacodylate buffer, and viewed under fluorescence and bright-field illumination.

Electron Microscopy: Cells were incubated with ASOR-gold (5 μg of adsorbed ASOR per ml in Medium 1, as calculated from the radioactivity of tracer ^{125}I-ASOR bound to the gold) at either 4°C or 37°C rinsed and reincubated at 37°C as described for the individual experiments. Cells were scraped from the dishes and pelleted in 2% glutaraldehyde in 120 mM sodium cacodylate buffer, pH 7.2. Cells were stained for acid phosphatase using β-glycerophosphate as substrate as described above, omitting the ammonium sulfide step. Cells were postfixed in 1% osmium tetroxide in 0.1 M veronal acetate buffer, pH 7.0, for 1 h and in some experiments were stained en bloc with uranyl acetate (50% of saturation in veronal buffer) for 30 min. The pellet was dehydrated by graded ethanol rinses and embedded in Epok resin (Ernest F. Fullam, Inc., Schenectady, NY). Ultrathin sections were cut on an LKB 2088 ultramicrotome (LKB Intruments, Inc., Gaithersburg, MD) and viewed either without further staining or after lead citrate counterstaining with a Jeol electron microscope at 80 kV.

RESULTS

Endocytic Vesicle pH

Both the excitation spectrum and the fluorescence intensity of fluorescein are extremely sensitive to changes in pH. Fluorescein-labeled macromolecules can be used as probes for the pH of specific intracellular compartments (15, 21, 31, 34). A calibration curve relating changes in the excitation profile to pH is shown in Fig. 1. When HepG2 cells were incubated with F-ASOR, in serum-free medium at 37°C for 10 min, rinsed and reincubated without F-ASOR for 5 min, the fluorescence was seen as a pattern of small dots, corresponding to endocytic vesicles, over a strong background of diffuse cellular autofluorescence (Fig. 2, *a* and *b*). On addition of 35 mM methylamine, a weak base which neutralizes acidic organelles (20, 21, 24), or of 20 μM monensin (an ionophore mediating Na^+/H^+ and K^+/H^+ exchange), there was a rapid increase in the intensity of the tiny dots and a large reduction of the 450/490 ratio of the dot fluorescence (Fig. 2, *c* and *d*). These changes in fluorescence are consistent with neutralization of an acidic environment. The small dots were not seen in cells exposed to F-ASOR in the presene of excess unlabeled ASOR (data not shown). When methylamine or monensin was added to cells which had not been exposed to F-ASOR or had been incubated with F-ASOR in the presence of a 20-fold excess of unlabeled ASOR, there was no change in the intensity of cellular autofluorescence (not shown). The observed changes in the F-ASOR fluorescence upon addition of methylamine or monensin indicate qualitatively that endocytic vesicles in HepG2 cells maintain an acidic internal pH.

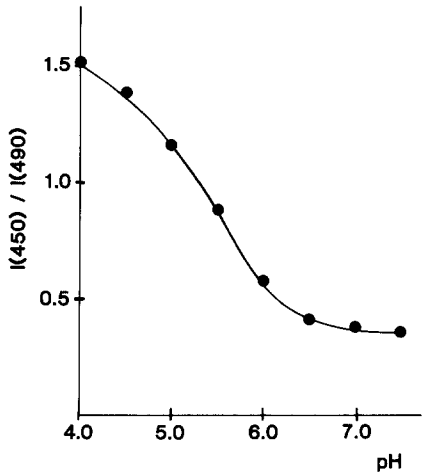

FIGURE 1 pH-dependence of F-ASOR fluorescence. F-ASOR (50 μg/ml) was buffered at pH 4.0, 4.5, 5.0, and 5.5 with 50 mM Tris-maleate. The solution at pH 6.0 contained 25 mM Tris-maleate and 25 mM sodium phosphate. Solutions at pH 6.5 and 7.0 were buffered with 50 mM sodium phosphate. The solution at pH 7.5 was buffered with 25 mM sodium phosphate and 25 mM Tris. Samples at each pH (10 μl in a hemocytometer) were placed on the inverted fluorescence microscope over a 63X primary objective. Fluorescence intensities were measured with excitation light passed through 450 nm and 490 nm narrow bandpass filters. As the pH increases there is an increase in the absolute fluorescence intensity and a decrease in the ratio of the intensities at the two wavelengths (the 450/490 ratio). The 450/490 ratio obtained with FITC-dextran is nearly identical with the curve shown.

Quantitative measurements of the pH within organelles can be made from measurements of fluorescein fluorescence at two wavelengths using a calibration curve (Fig. 1). However, when we tried to apply previously used methods to HepG2 cells, we found that the high level of cellular autofluorescence made meaningful measurements impossible. As described in this section, we could overcome this problem by using digital image processing to measure fluorescence intensities only from the bright dots corresponding to endocytic vesicles. Computer algorithms were developed for subtracting out the autofluorescence and for comparing the intensities of individual dots (vesicles) at 450 nm and 490 nm excitation. From the ratio of intensities at 450 nm and 490 nm, the pH of individual vesicles could be estimated.

Video images of the cells were digitized as described in Materials and Methods. The autofluorescence was estimated as the median intensity (50th percentile) within each 32 pixel × 32 pixel region, and this autofluoresence contribution was subtracted from all pixel intensities, with resulting negative intensities set to zero. Bright spots, corresponding to individual endocytic vesicles or small groups of closely spaced vesicles, were identified and catalogued by a computer algorithm. In this algorithm, adjacent pixels with intensities above a threshold value were grouped together into spots, and the total intensity within each spot and its coordinates were tabulated and stored on a disk file. For all cases, the coordinates for the spots were first determined using the images obtained with 490-nm excitation. The intensities of exactly

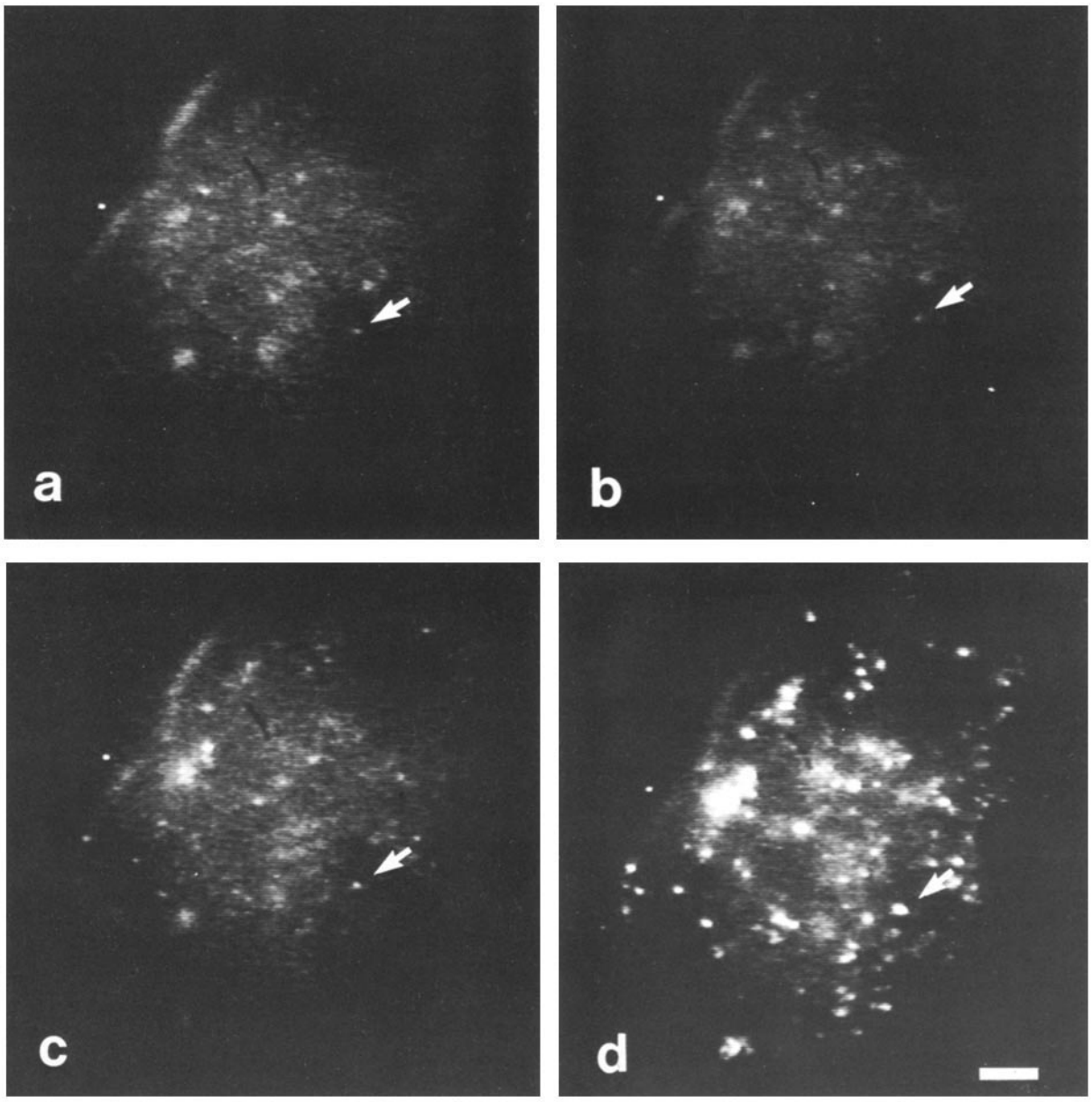

FIGURE 2 Fluorescence images of HepG2 cells that have endocytosed F-ASOR. Cells grown on coverslip-bottom dishes were incubated in the presence of F-ASOR (100 μg/ml; 50 K_d) in αMEM containing 2 mg/ml of bovine serum albumin for 10 min at 37°C, rinsed with PBS containing 1 mM calcium chloride at 23°C and transferred to the inverted fluorescence microscope. Fluorescence images with excitation at 450 nm (*a* and *c*) ad 490 nm (*b* and *d*) were recorded on videotape before (*a* and *b*) and 2 minutes after (*c* and *d*) the addition of 20 μM monensin. In cells before the addition of monensin (*a* and *b*) the punctate F-ASOR fluoresence is weak due to the low vesicle pH and in some areas is only marginally visible over the cellular autofluorescence. In this group of cells one vesicle (arrow) is present over a region of low autofluorescence and is therefore particularly well resolved. Monensin, a monovalent cation ionophore, induces a rapid and dramatic increase in the punctate fluorescence, accompanied by a decrease in the 450/490 ratio which, by reference to Fig. 1, indicates a neutralization of the vesicle pH. Images were digitized, and the 450/490 ratios of several dots were measured after subtraction of the local autofluorescence component (see Fig. 3). Bar, 4 μm.

the same pixels were determined from the 450-nm image, and the 450/490 ratio for each spot was determined. Threshold values were used only to select the pixels which would be considered in the 450/490 ratio. The specific value used was determined by visual inspection of the image showing only pixels above the threshold intensity. Since the same pixels were measured in both images, the total intensity ratio is relatively insensitive to the threshold value used. (This is discussed in detail below.) One set of cells used for the spot intensity ratio measurement is shown in Fig. 2. Reference to a standard curve (Fig. 1) provided a measure of vesicle pH. The effects of the image processing steps are shown in Fig. 3.

The validity of measuring pH values from individual spots was checked using human fibroblast cells fixed and placed in buffers at various pH values after uptake of F-α_2M. Images were processed as described above, and the 450/490 ratios of individual spots of fluorescence were determined. The curve of I_{450}/I_{490} vs. pH agreed well with the curve shown in Fig. 1

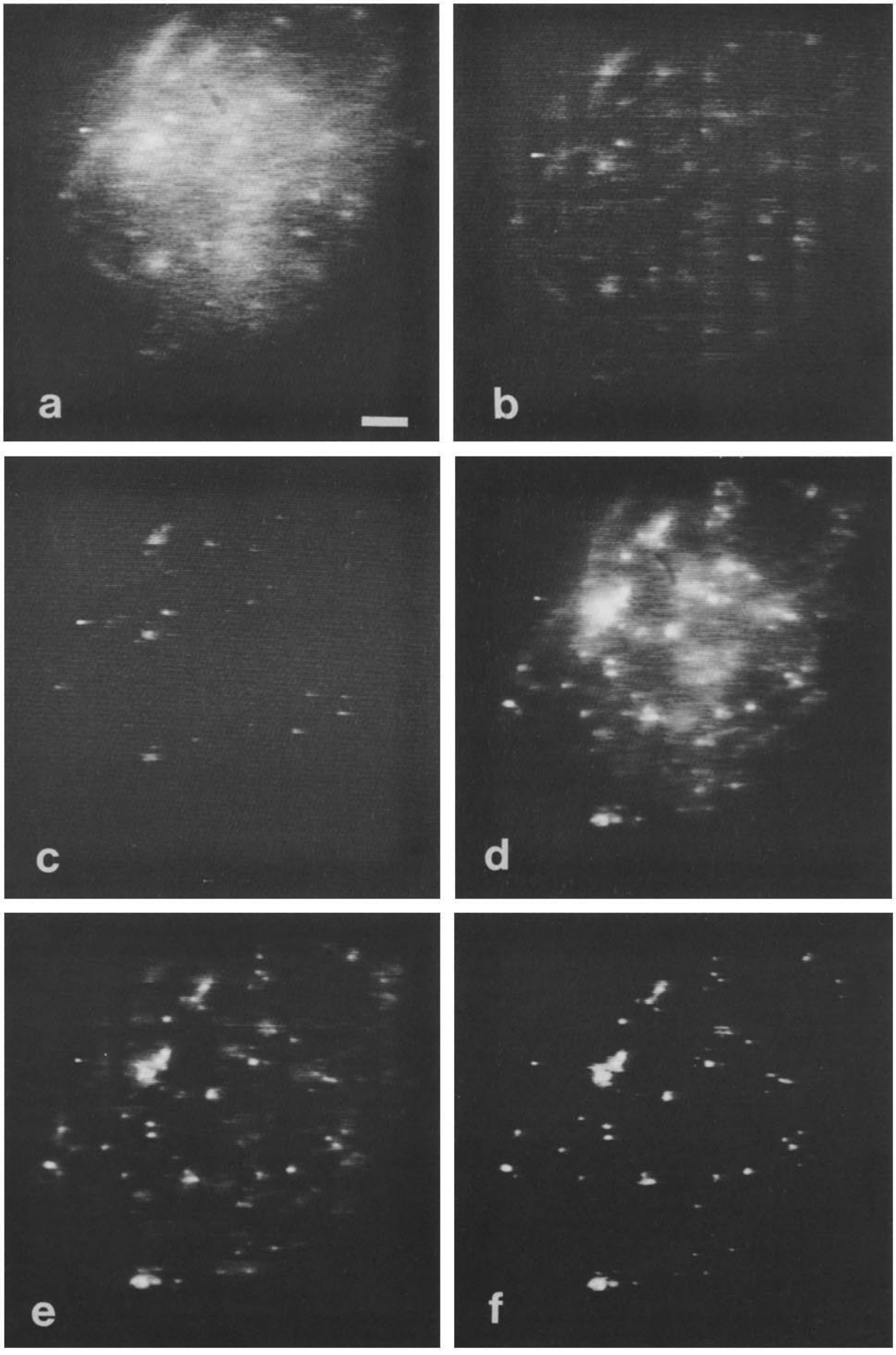
a
b
c
d
e
f

TABLE I

*Effect of Image Processing Parameters on I_{450}/I_{440} for Endocytic Vesicles**

Monensin concentration	Intensity percentile for autofluorescence subtraction‡	Threshold intensity for inclusion in spots§	Number of pixels above threshold	Average I_{450}/I_{490}‖	pH
(μM)					
0	50	11	1,206	1.00	5.3
0	50¶	13¶	673	1.01	5.3
0	50	16	326	1.01	5.3
0	25	16	667	1.06	5.2
0	75	10	617	0.89	5.4
20	50	21	3,707	0.34	>7.0‡‡
20	50**	30**	1,845	0.32	>7.0
20	50	41	934	0.32	>7.0
20	25	36	1,861	0.36	>7.0
20	75	22	1,786	0.27	>7.0

* Cells were incubated with F-ASOR as described in Fig. 2, and the digitized images shown in Fig. 3, *a* and *d*, were processed in various ways to determine the extent to which values of processing parameters affected the value of I_{450}/I_{490}. The portion of the image used for analysis contained 147,456 pixels.

‡ The image was divided into 32 × 32 pixel segments, and the contribution from autofluorescence and other "background" light sources was determined within each segment. This background component was defined as the 25th, 50th, or 75th percentile of intensity, and this background value was subtracted from all pixel intensities within that segment. The table shows the effects of varying the percentile used while keeping the number of pixels measured nearly constant.

§ After subtracting the background, a single threshold value was used for the whole image. Threshold values were chosen so that measurements of the 450/490 ratio would be restricted mainly to bright dots observed with 490-nm excitation. The choice was based on visual inspection of the images, after removing pixels below the threshold. The table shows the effects on pH values of varying the threshold intensity with a resulting change in the number of pixels included in the measurement.

‖ After applying the indicated image processing steps to the image with 490-nm excitation, the total intensity of all the pixels above the threshold the 450 nm image, and the sum of the intensities of exactly the same pixels was determined. The 450/490 ratio for the entire image is shown.

¶ These are the values used for Fig. 3, *a–c*.

** These values were used for Fig. 3, *d–f*.

‡‡ Fluorescein is not an accurate pH indicator above pH 7.

(i.e., all of the average values were within 0.2 pH units of the values for whole cell measurements). There was relatively large uncertainty in pH measurements from individual endocytic vesicles. At pH 4.5 the standard deviation in I_{450}/I_{490} was ± 0.25, and at pH 5.5–6.5 the standard deviation was ± 0.1. These values indicate that pH measurements from a *single* vesicle have a standard deviation of ~0.3–0.5 pH units.

For the 27 brightest dots in the image shown in Fig. 3 *c*, obtained before monensin treatment, the average value of the 450/490 ratio was 0.92 (±0.3) corresponding to a pH of 5.4. The standard deviation probably represents, to a large extent, uncertainties in the measurement of individual vesicle intensities; we cannot determine the variability in endocytic vesicle pH from these measurements. When two similar fields were analyzed by the same procedures, the average values for the 450/490 ratio were 0.93 (±0.1) and 0.8 (±0.2) corresponding to pH values of 5.4 and 5.5. When monensin (20 μM) was added to the culture medium, the average value of the 450/490 ratio for the 38 brightest dots in Fig. 3 *f* was 0.31 (±0.1), corresponding to a pH between 7.0 and 7.4.

The values used to determine autofluorescence levels and intensity threshold levels are somewhat arbitrary, so it was necessary to determine whether the 450/490 ratio was sensitive to the values chosen. The results of varying the threshold values and autofluorescence values are shown in Table I. First, with the autofluorescence value set at the median (50th percentile) intensity, the threshold value was changed to double or halve the number of pixels used for the measurement of the 450/490 ratio. Second, the autofluorescence value within each 32 × 32 region was set at the 25th percentile or the 75th percentile intensity and the threshold was set so that approximately the same number of pixels were used in each measurement of the 450/490 ratio. As shown in Table I, none of these changes produced a significant alteration in the 450/490 ratio for cells in the presence or absence of monensin. This indicates that the values of the 450/490 ratio are relatively independent of the parameters used in the image processing and represent a valid method for estimating the pH of endocytic vesicles.

As a confirmation of the method, and to make sure that there was not a diffuse component of F-ASOR at neutral pH, the endocytic vesicle pH was also measured by making total fluorescence intensity measurements with the microscope spectrofluorometer with excitation at 450 and 490 nm from groups of two or three cells before and after the cells had endocytosed F-ASOR. Since the entire experiment was carried out on the microscope stage, the autofluorescence signal could be measured before the cells were exposed to F-ASOR and then subtracted as background. In a series of five experiments, the specific F-ASOR fluorescence averaged 21% of the total signal with excitation at 490 nm and 12% at 450 nm. The 450/490 ratio after a 10-min pulse and a 5-min rinse was 1.00

FIGURE 3 The images of the cells shown in Fig. 2 were digitized and processed for the measurement of fluorescence intensity of endocytic vesicles. (*a–c*) 490-nm excitation before monensin treatment. (*d–f*) 490-nm excitation after monensin treatment. Eight video frames of each image were digitized and averaged (*a* and *d*). The images were divided into 32 pixel × 32 pixel regions, and the median (50th percentile) intensity was defined as background. This value was subtracted from all pixel intensities (*b* and *e*). To identify dots within the image, a threshold intensity was chosen. Pixels above this threshold intensity were used for intensity measurements. The threshold values for cells before or after monensin treatment were 13 and 30, respectively (*c* and *f*). The images shown in *a–c* have been printed with a brief exposure time to allow better visualization of dim spots and background autofluorescence. Bar, 4 μm.

(±0.21) (Table II), which by reference to the standard curve (Fig. 1) indicates an endocytic vesicle pH of 5.3 (±0.3). The 450/490 ratio did not change significantly when cells were incubated for an additional 5 min, indicating that acidification is complete at early times. As expected, when cells were fixed and exposed to methylamine to dissipate any remaining pH gradients, the 450/490 ratio fell to 0.31 (±0.09), indicating neutralization of the F-ASOR microenvironment. Although the background fluorescence levels were high relative to the fluorescein signal, measurements of the intensity within a field were highly reproducible (±1%) so that accurate corrections could be made. Addition of methylamine or monensin produced no detectable change in the cellular autofluorescence with 450- or 490-nm excitation.

The values of the vesicle pH obtained by whole cell measurements (Table II) and digital image analysis (Table I) are in excellent agreement. It is possible that there is a diffuse component of internalized F-ASOR which could not be detected by the image analysis. If that is the case, this component must be relatively small or have the same pH as the punctate component shown in Fig. 3.

Although these measurements were carried out at 37°C, qualitatively similar findings were obtained when both the uptake of F-ASOR and the observations were carried out at 23°C. There was a dramatic increase in punctate F-ASOR fluorescence on addition of methylamine to cells incubated at 23°C (data not shown), indicating that endocytic vesicle acidification is not highly temperature-dependent in this range.

Lysosomal pH

Fluoresceinated dextran (FITC-dextran), which is taken up by cells during pinocytosis and accumulates in secondary lysosomes where it is not degraded, has been used as a probe for the internal pH of lysosomes in macrophages (21, 24), fibroblasts (1), and hepatocytes (22). We used FITC-dextran to compare the pH of lysosomes with the pH of endocytic vesicles.

When HepG2 cells were incubated overnight in the presence of FITC-dextran (40,000 mol wt) at 2 mg/ml, rinsed in PBS containing 1 mM calcium chloride and viewed by fluorescence microscopy (not shown), the FITC-dextran was localized within the cell in large (1–2 μm) round structures (approximately three per cell) which were often perinuclear in location. We have identified these structures as secondary lysosomes, based on previous studies where the same technique was applied to macrophages (21, 24) and hepatocytes (22).

The internal pH of secondary lysosomes that had accumulated FITC-dextran was measured by analyzing fluorescence images of cells with excitation centered first at 450 nm and then at 490 nm. Video images of cells incubated with FITC-dextran were digitized and processed as described above. Values of the 450/490 ratio for individual lysosomes were obtained, and a histogram of these 450/490 values is shown in Fig. 4. The distribution centers around pH 5.0, but a small population of FITC-dextran containing structures have neutral pH values. Addition of methylamine (35 mM) results in a rapid increase in the fluorescence intensity and a shift of the lysosomal pH distribution to neutrality (Fig. 4) as has been reported by Ohkuma and Poole for macrophage lysosomes (21, 24).

TABLE II

*pH of the F-ASOR Microenvironment in Living and Fixed Cells**

Experiment	Conditions	450/490 ratio‡	pH
1	10-min continuous uptake/rinse/5 min further incubation	1.00 ± 0.21 (n = 5)	5.3 ± 0.3
2	10-min continuous uptake/rinse/10-min further incubation	1.09 ± 0.22 (n = 5)	5.2 ± 0.3
3	10-min continuous uptake/rinse/5-min further incubation/fix/rinse/add methylamine§	0.31 ± 0.09 (n = 5)	>7.0‖

* HepG2 cells grown on coverslip-bottom dishes were rinsed in Medium 1 at 37° and transferred to the microscope stage, maintained at 37°C by an air curtain heater. The autofluorescence from a group of two or three cells was measured with excitation at 450 and 490 nm and subtracted from subsequent measurements as background. Phase-contrast and fluorescence images were observed on the video monitor to ascertain that the field did not shift in subsequent rinses. Cells were incubated with F-ASOR (100 μg/ml) in medium 1 for the indicated times. In experiment 3 the cells were fixed for 10 min in 2% formaldehyde in PBS containing 1 mM calcium chloride and rinsed with PBS containing 30 mM methylamine.

‡ Defined as the ratio of F-ASOR fluorescence intensity with excitation at 450 nm to that with excitation at 490 nm.

§ The autofluorescence signal, measured from cells not exposed to F-ASOR, did not change on addition of methylamine (signal stable within 1 percent in both of two experiments).

‖ The F-ASOR is not sensitive as a pH probe at pH > 7.0 (Fig. 1).

Acidic Endocytic Vesicles Lack Lysosomal Characteristics

Biochemical and morphological studies were carried out to determine whether endocytic vesicles had lysosomal proper-

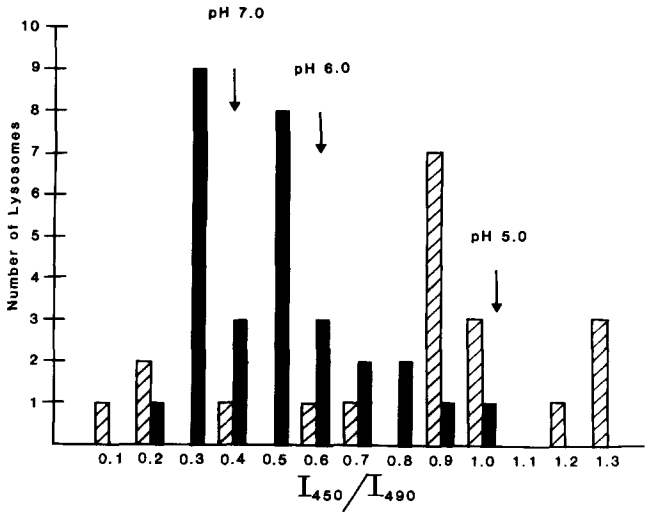

FIGURE 4 Histogram of the internal pH of individual secondary lysosomes. HepG2 cells were incubated with FITC-dextran and fluorescence images were digitized and processed as described in the text. The pH of individual lysosomes was derived from the ratio of fluorescence intensities with excitation at 450 and 490 nm. Before addition of methylamine the distribution of lysosomal pH centers near pH 5.0; after the addition of methylamine (35 mM) the lysosomal pH gradient is dissipated, and the distribution shifts to neutrality. A small number (~25%) of FITC-dextran-containing structures do not maintain an acidic internal pH even before the addition of methylamine. Solid bars, after MA; striped bars, before MA.

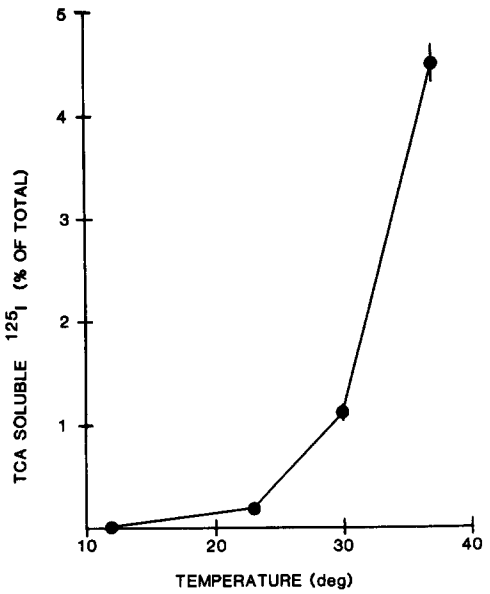

FIGURE 5 Temperature dependence of ^{125}I-ASOR degradation by HepG2 cells. Cells were incubated with ^{125}I-ASOR (1.0 μg/ml) in medium 1 for 15 min at 37°C, rinsed and reincubated in medium 1 at the indicated temperatures for 60 min. The medium was drawn off and precipitated with 10% trichloroacetic acid. Cells were overlayed with 10 percent trichloroacetic acid which was drawn off after 5 min. Total trichloroacetic acid-soluble radioactivity was defined as that found in the medium and extracted from the cells. The total cell-associated trichloroacetic acid-precipitable radioactivity after the reincubation at 37°C was equivalent to 0.038 μg of ^{125}I-ASOR per 10^6 cells or approximately 60,000 molecules per cell. The degradation of ^{125}I-ASOR is highly temperature dependent: degration is inhibited by 90% as the temperature is dropped from 37°C to 23°C.

ties. Our pH measurements were made 15 min after the initial exposure to F-ASOR. As shown in Fig. 5, further incubation for 60 min at 37°C results in the degradation of only 5% of the cell-associated ASOR. This slow degradation is consistent with the kinetic analysis of Schwartz et al. (26). At 23°C, a temperature at which we also observed acidification, <1% of the cell-associated ASOR was degraded in 60 min. These results demonstrate that acidification occurs in structures which are essentially devoid of proteolytic activity on ASOR.

To further characterize the acidic endocytic vesicles, we carried out cytochemical studies using light and electron microscopy with F-ASOR or ASOR adsorbed to 10–20-nm colloidal gold particles as tracers. For light microscopy, cells were incubated with F-ASOR according to the conditions of Table II (a 10-min incubation and a 5-min rinse) and were then fixed and stained for acid phosphatase activity. The reaction product was seen in lysosomes concentrated about the nucleus but also found in structures throughout the cytoplasm. It is clear from comparison of the bright-field and fluorescence images that at this time the F-ASOR is not in lysosomes which can be seen at the light microscope level (Fig. 6).

For electron microscopy, cells were incubated with ASOR-gold at 37°C for 10 min, rinsed and reincubated for an additional 5 or 50 min. Cells were fixed and stained for acid phosphatase with β-glycerophosphate as substrate. After a 10-min pulse and a 5-min rinse the tracer was found almost exclusively in vesicles that did not contain detectable acid phosphatase activity. These structures were both univesicular and multivesicular (~75% appeared to be multivesicular) and sometimes gave off single or multiple tubular extensions (Fig. 7). Acid phosphatase activity was concentrated in Golgi cisternae and small vesicles (Fig. 7) and in rare large secondary

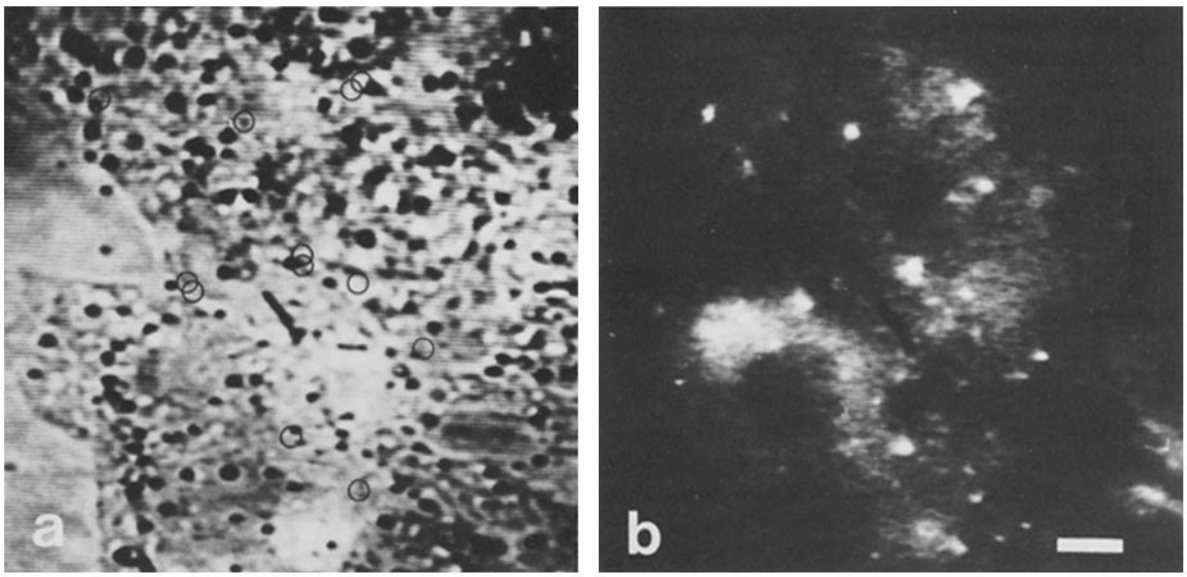

FIGURE 6 Cytochemical localization of acid phoshatase in HepG2 cells which have endocytosed F-ASOR. Cells were incubated with F-ASOR under the conditions of experiment 1, Table I, fixed and stained for acid phosphatase activity using β-glycerophosphate as the substrate. Cells were observed by bright-field illumination (*a*) and by fluorescence (*b*). The images were aligned by reference to the original videotape. Lysosomes are concentrated about the nucleus, but are found throughout the cell. A tracing of dots in the fluorescence image (open circles in *a*) cannot be superimposed over acid phosphatase reaction product in the bright-field image. This is consistent with a prelysosomal location for the internalized F-ASOR. Bar, 3 μm.

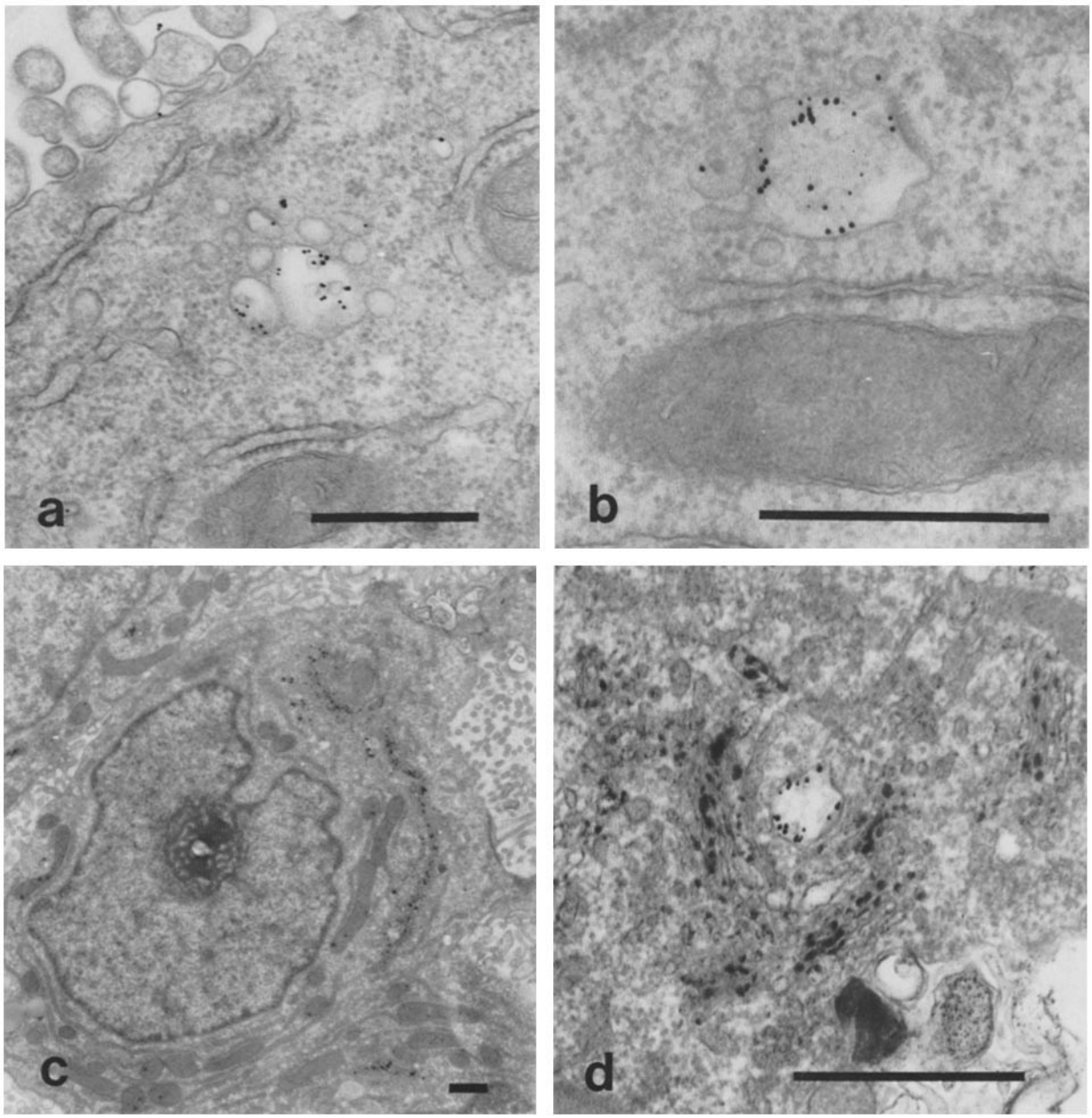

FIGURE 7 Ultrastructural and cytochemical characterization of endocytic vesicles containing ASOR-gold. HepG2 cells were incubated with ASOR adsorbed to 10–20 nm gold particles (5 μg of adsorbed ASOR per milliliter) at 37°C for 10 min, rinsed, reincubated for 5 min, fixed and processed for electron microscopy as described in the text. Gold particles were found in vesicles near the plasma membrane (*a*) which were often multivesicular (*a* and *b*) and sometimes gave off tubular extensions (*b* and *d*). The vesicles were often seen clustered in groups (*a* and *b*), suggesting the possibility of fusion events. When cells were stained for acid phosphatase (*c* and *d*) the reaction product was seen associated with vesicles and cisternae of the Golgi apparatus (GERL). The endocytic vesicles containing gold particles did not contain detectable acid phosphatase activity (*d*). Of 1,000 gold particles found intracellularly, only two were seen in a small acid phosphatase-positive lysosome. Bar, 0.5 μm.

lysosomes (not shown). Out of 1,000 gold particles counted in approximately 20 sections (two blocks), two particles were seen in a small acid phosphatase-positive structure and 998 were seen in endocytic vesicles which did not contain detectable enzyme activity. When cells were reincubated for 50 min after rinsing, gold particles were seen in multivesicular bodies that were often positive for acid phosphatase activity (Fig. 8). Of 678 particles counted in approximately 20 sections (two blocks), 170 were in acid phosphatase-positive structures and 498 were in multivesicular bodies which did not show detectable reaction product. This result correlates well with the kinetics of ^{125}I-ASOR degradation, which is just beginning at this time (Fig. 6; reference 26).

No gold particles were seen intracellularly in 10 sections of cells which were incubated with ASOR adsorbed to colloidal gold in the presence of 1 mg/ml of free ASOR.These cytochemical data and the kinetics of ligand internalization and degradation demonstrate that the pH measurements with F-ASOR were made when the F-ASOR was in prelysosomal endocytic vesicles. We cannot, of course, rule out the presence

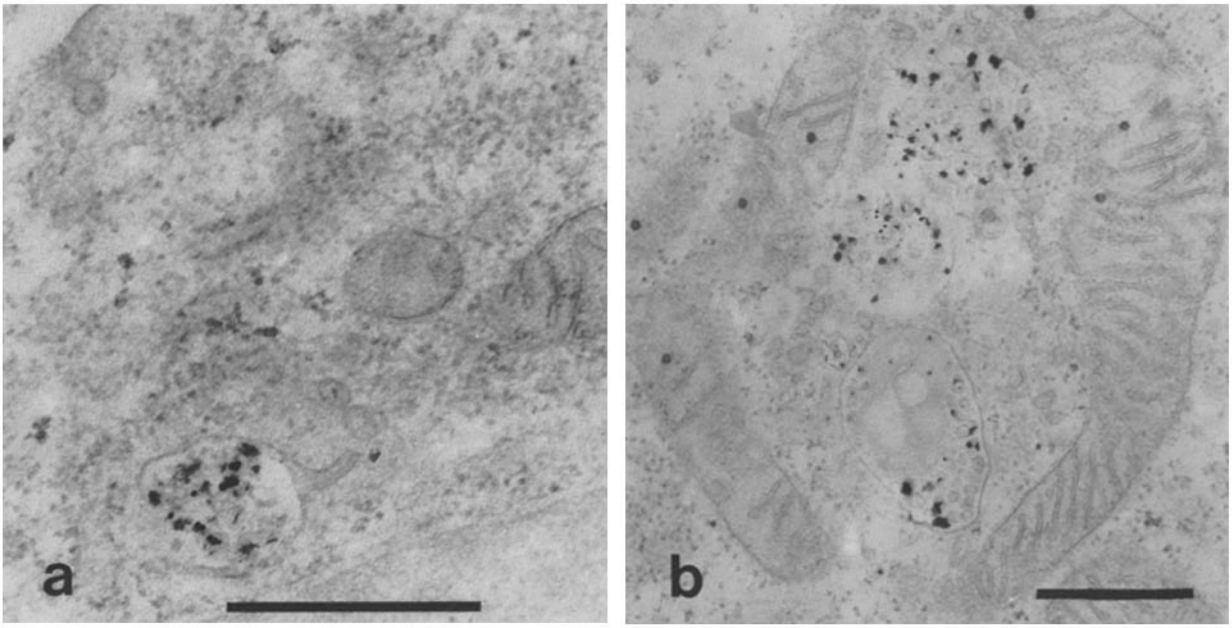

FIGURE 8 Gold particles visualized in secondary lysosomes after a 1 h incubation. HepG2 cells were incubated with ASOR-gold as in the experiment of Fig. 7, but were reincubated at 37°C for 50 min. Of 678 gold particles found intracellularly, 170 were in structures which contained acid phosphatase reaction product (*a* and *b*). These lysosomes were multivesicular (*a* and *b*) and occasionally gave off tubular extensions (*a*). Thus, morphological criteria are not sufficient to distinguish endocytic vesicles from lysosomes; cytochemical characterization is essential. Movement of gold particles into lysosomes correlates well with the kinetics of ^{125}I-ASOR degradation, which is beginning at this time (reference 26 and Fig. 5). Bar, 0.5 μm.

in these structures of very small amounts of lysosomal enzymes not detectable either by cytochemical staining methods or by the degradation of ASOR.

Correlation between Endocytic Vesicle pH and Ligand and Receptor Processing

Various manipulations of cells have been reported to affect certain steps in the receptor-mediated endocytosis pathway. We carried out several of these manipulations under conditions in which we have also measured the pH of endocytic vesicles or lysosomes to determine whether the effects can be linked to endocytic vesicle acidification.

As shown in Fig. 5, degradation of ASOR is almost completely inhibited by dropping the temperature to 23°C, in agreement with the report of Dunn et al. (9) for the perfused liver at 20°C. In sharp contrast to the marked temperature-dependence of ligand degradation, the rate of receptor recycling was only slightly reduced when the temperature was shifted from 37°C to 23°C (Fig. 9). To measure the rate of receptor recycling, we first incubated cells at 37°C for 10 min with a saturating concentration of unlabeled ASOR and then rinsed at either 37°C or at 23°C and incubated further for the indicated times. The number of receptors that had returned to the surface (i.e., recycled) after a given amount of time was indicated by the amount of ^{125}I-ASOR which bound to the cells at 4°C. Previous studies (26) have demonstrated that HepG2 cells do not maintain a large intracellular pool of receptors. Therefore, this experiment measures true recycling and not insertion into the plasma membrane of receptors derived from an intracellular pool. The rate of recycling during the first 5 min after rinsing was only slightly reduced at 23°C compared to 37°C. Full recovery of binding sites occurred at 37°C, but at 23°C binding reached only 83% of the initial level.

The rapid recovery of surface binding sites implies that, even at 37°C, recycling of receptors is not coupled to ligand degradation. A shift to 23°C uncouples the two processes even more dramatically and lends further support to a model in which receptor-ligand dissociation occurs in the acidified endocytic vesicle and is followed by rapid recycling of unoccupied receptors back to the plasma membrane. Since endocytic vesicles and lysosomes remain acidic at 23°C, the temperature dependent inhibition of ligand degradation is not due to changes in pH of these organelles.

When HepG2 cells were exposed to methylamine or monensin at concentrations that dissipate the endocytic vesicle pH gradient, there was a rapid loss of asialoglycoprotein receptors from the cell surface (Fig. 10). In these experiments cells were preincubated for 10 min in either the presence or absence of ligand and with or without methylamine (35 mM), then rinsed and reincubated for 10 min either with or without methylamine. Surface binding sites were measured by incubating cells with ^{125}I-ASOR at 4°C. As shown in Fig. 10, the methylamine-induced loss of surface receptors appeared to be greater when ligand was present during the preincubation. However, when cells were rinsed briefly with 5 mM EDTA at 4°C before addition of the ^{125}I-ASOR, the amount of binding increased to the level of cells which were not exposed to ligand during the preincubation. Since EDTA releases surface-bound ASOR (26), this implies that the difference in apparent surface binding sites was due to a small percentage of receptors that remained occupied and on the surface after the preincubation and rinse. Therefore, the methylamine-induced loss of surface receptors is essentially independent of the presence of ligand. A similar ligand-independent loss of receptors was induced by monensin (20 μM).

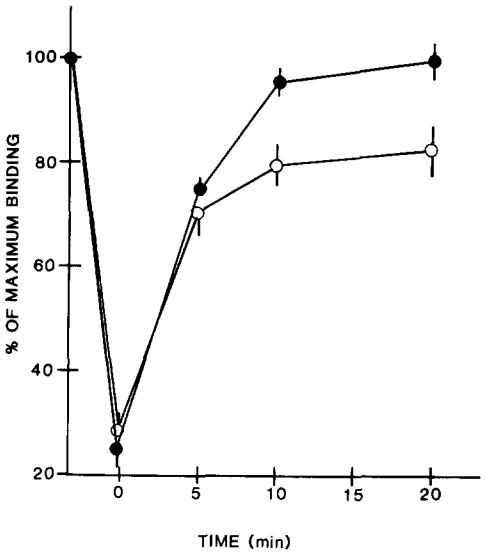

FIGURE 9 Temperature-dependence of the rate of reappearance of unoccupied receptors at the plasma membrane after endocytosis of ASOR. Cells were incubated for 10 min at 37°C in the presence of unlabeled ASOR (20 μg/ml; 10 K_d) in medium 1. Cells were then rinsed at 23°C (○) or 37°C (●) and reincubated at these temperatures for the indicated times. The number of unoccupied receptors at the plasma membrane was measured by exposing cells to ^{125}I-ASOR (1 μg/ml) at 4°C for 1 h and measuring total cell-bound radioactivity. Since HepG2 cells do not maintain a significant pool of intracellular receptors (26) this experiment measures receptor recycling. The rate of receptor recycling was not highly temperature dependent between 37°C and 23°C.

Receptor loss induced by methylamine was reversible. When cells were incubated with methylamine for 15 min, rinsed, and reincubated in the presence of cycloheximide (20 μg/ml), the number of surface binding sites returned to control levels within 1 h (Fig. 11). In contrast, the loss of surface receptors induced by monensin was not reversible under these same conditions (Fig. 11). It was possible that the irreversible loss of receptors induced by monensin resulted from an inability of the endocytic vesicles to re-acidify after monensin treatment. However, as shown in Fig. 12, the increase in endocytic vesicle pH caused by monensin is rapidly reversed when the monensin is removed from the medium. This re-acidification was also observed at 23°C. Similar reversibility was reported previously for mouse fibroblast endocytic vesicles (20).These results suggest that monensin affects receptor distribution by more than one mechanism. While the effect on endocytic vesicle pH is rapidly reversible, the effect on the second site is not. We do not know the identity of the second site of action, but it is known that monensin affects the Golgi complex (29) at lower concentrations than are required to raise the pH of endocytic vesicles (20).

To determine whether vesicle acidification is required for internalization of prebound ligand, we allowed ^{125}I-ASOR to bind to cells at 4°C and then measured the rate of its disappearance from the surface upon warming the cells to 30°C, in either the presence or absence of methylamine. Surface-bound ligand was defined as EDTA-releasable ^{125}I-ASOR. Methylamine (35 mM) did not dramatically inhibit internalization of prebound ligand (data not shown). More than half of the ligand became resistant to release by EDTA within 3 min whether in the presence or absence of methylamine. However, the rate of internalization was slightly slower in the presence of methylamine (~20% difference in surface bound ligand after 9 min, statistically significant in both of two experiments). Similar results were obtained when monensin was used in place of methylamine (data not shown).

If neutralization of the vesicle pH by methylamine were to block ligand-receptor dissociation without preventing the recycling of occupied receptors, then we might expect to be able to release ligand that had been internalized in the presence of methylamine by incubating cells continuously in the presence of methylamine and EDTA. This type of behavior has been reported by Tietze et al. (30) for the mannose receptor in macrophages. In our system, this experiment yielded a negative result: when cells were allowed to internalize ^{125}I-ASOR in the presence or absence of methylamine (4 min at 30°C), rinsed and reincubated for 10 min in the presence or absence of methylamine and in the presence of EDTA, the amount of ligand released into the medium was the same in experimental and control dishes (data not shown). This is consistent with a model in which methylamine blocks both ligand-receptor dissociation and receptor recycling to the cell surface.

Bridges et al. (6) have developed a precipitation assay for determining the extent to which intracellular ASOR is bound to its receptor. We used their procedure to follow the kinetics of intracellular dissociation of ASOR from its receptor. As

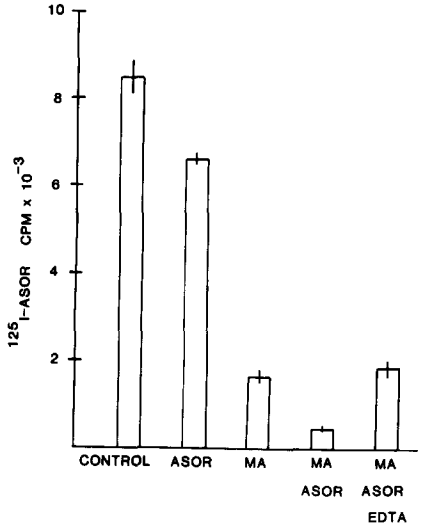

FIGURE 10 Methylamine induces a ligand-independent loss of surface receptors for ^{125}I-ASOR. HepG2 cells were incubated for 10 min at 37°C in the presence or absence of unlabeled ASOR (20 μg/ml; 10 K_d) in medium 1 and in the presence or absence of methylamine (*MA*; 30 mM) as indicated in the figure. Cells were rinsed and reincubated for 10 min at 37°C in the absence of ASOR. When methylamine was present during the initial incubation it was also present during the reincubation. Cells were then rinsed with medium 1 at 4°C. Some dishes were exposed to EDTA (5 mM in PBS) at 4°C for 5 min to remove surface-bound ASOR. Cells were exposed to ^{125}I-ASOR (μg/ml) for 1 h at 4°C to measure the number of unoccupied receptors at the plasma membrane. Methylamine induced a 75% loss of surface receptors. Incubation with ASOR in the absence of methylamine resulted in a loss of <25% of unoccupied surface receptors. While the presence of ligand during the initial incubation appeared to augment the methylamine-induced receptor loss; this was totally attributable to persistent occupancy of surface receptors by unlabeled ASOR. This was shown by the effect of EDTA treatment, which returned the number of binding sites to the level observed when methylamine alone was present during the initial incubation.

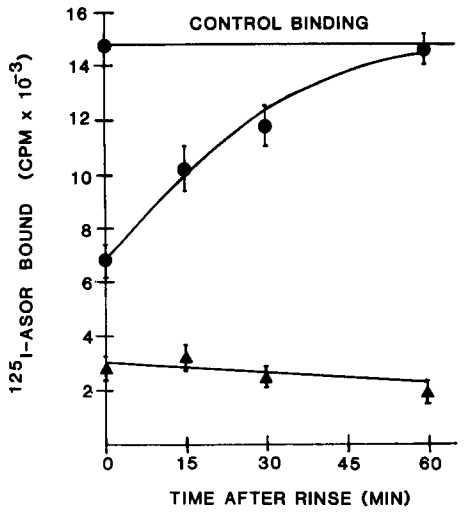

FIGURE 11 Reversibility of methylamine and monensin induced receptor loss. Cells were preincubated in medium 1 at 37°C for 10 min in the presence or absence of 30 mM methylamine (circles) or 20 mM monensin (triangles). Cells were then rinsed either in medium 1 at 4°C (zero time point) or in αMEM containing 10% fetal bovine serum and 10 μg/ml cycloheximide and incubated at 37°C for the indicated times. The recovery of surface ASG receptors was measured by exposing cells to ^{125}I-ASOR (1 μg/ml) in medium 1 at 4°C for 1 h and counting the total cell-associated radioactivity. While both methylamine and monensin induced a profound loss of surface receptors, only the methylamine-induced loss was reversible. Recovery from methylamine was complete within 1 h in the presence of cycloheximide, implying that the recovery does not depend on synthesis of new receptors.

shown in Fig. 13, by 6 min after warming, 60% of the ^{125}I-ASOR has dissociated from its receptor (i.e., dissociation occurs in endocytic vesicles). When cells are warmed to 37°C in the presence of 20 μM monensin, ligand is fully internalized within 6 min (data not shown), but ligand-receptor dissociation is completely blocked. This experiment provides direct biochemical evidence in support of a crucial role for vesicle acidification in driving ligand-receptor dissociation. Harford et al. (14) have recently made similar observations in the isolated hepatocyte system.

The observation that monensin blocks dissociation of prebound ligand from its receptor while allowing internalization to proceed at approximately the normal rate suggested that we might be able to localize "trapped" intracellular ligand receptor complexes at the ultrastructural level. Cells were preincubated with ASOR-gold at 4°C to allow binding to the cell surface and then warmed to 37°C in the presence or absence of 20 μM monensin to allow internalization. At 10 min after warming to 37°C, the gold particles in both monensin-treated and control cells were found predominantly in noncoated endocytic vesicles (Fig. 14). In monensin-treated cells, but not in controls, cisternae of the Golgi apparatus were markedly dilated (not shown). These results indicate that monensin, at concentrations that raise the endocytic vesicle pH and that block ligand receptor dissociation, does not block the transfer of ligand from the cell surface through coated structures to noncoated endocytic vesicles. The exact location of the primary site of the monensin-induced block in receptor recycling remains to be determined; but it is either at the level of the endocytic vesicle or further along the recycling pathway.

DISCUSSION

Our observation that endocytic vesicles in mouse fibroblasts are acidic organelles (31) prompted us to suggest that rapid

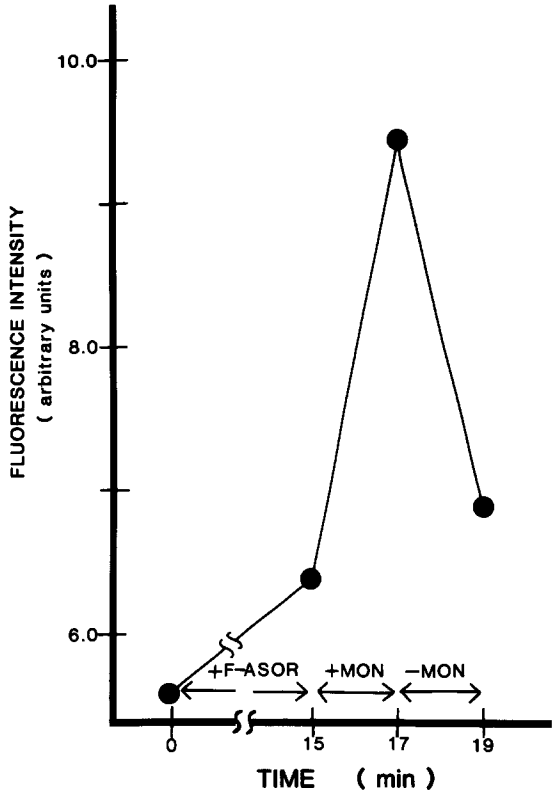

FIGURE 12 Endocytic vesicles rapidly reacidify after removal of monensin. HepG2 cells, grown on polylysine-treated coverslip-bottom dishes, were rinsed with medium 1 and placed on the inverted fluorescence microscope stage, maintained at 37°C by an air curtain heater. Isolated groups of three or four cells were visualized and their position outlined on the video monitor screen. The autofluorescence intensity at 490-nm excitation was measured with the photomultiplier tube at the beginning of the experiment. The medium was then drawn off and replaced with medium 2 containing 50 μg/ml of F-ASOR. After 10 min, the dish was rinsed four times with medium 1. After an additional 5 min, the fluorescence intensity was measured. Monensin was then added to a final concentration of 20 μM and the intensity was measured after 2 min. The monensin was then washed out by rinsing with medium 1 and the intensity was measured again after 2 min. Addition of 20 μM monensin results in an increase in the pH of endocytic vesicles from approximately 5.3 to 7.0 (Table I). As the pH increases, the fluorescence intensity with 490-nm excitation increases, and changes in intensity can be used to monitor changes in pH (20, 21, 24). The pH dependence of the intensity of fluorescein-labeled ligands as measured with our instrument has been reported (20). Changes in intensity were measured in this experiment rather than the 450/490 ratio to minimize the exposure of the cells to light during the experiment. While accurate pH values cannot be determined from single wavelength measurments, the observed rise in intensity is consistent with the changes in pH (5.3 to 7.0) reported in Table I. Dissipation of the vesicle pH gradient by monensin is indicated by the rapid increase in F-ASOR fluorescence intensity. (Addition of monensin to control cells not exposed to F-ASOR did not change the intensity of cellular autofluorescence.) The effect of monensin is fully reversed within 2 minutes of washing out the drug. The rise and fall of the fluorescence intensity coincided with an increase and decrease in the brightness of endocytic vesicles as observed on the video monitor. This result indicates that endocytic vesicles in HepG2 cells can actively maintain an acidic internal pH.

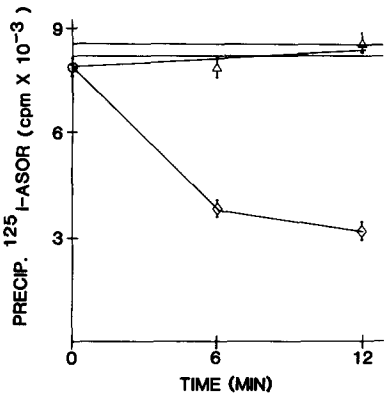

FIGURE 13 Monensin blocks ligand-receptor dissociation. HepG2 cells grown in 35-mm dishes were exposed to ^{125}I-ASOR (1 μg/ml) in medium 1 at 4°C for 1 h either in the presence or absence of excess unlabeled ASOR (500 μg/ml). The dishes were rinsed at 4°C and Dulbecco's modified Eagle's medium containing 2 mg/ml bovine serum albumin was added, either with or without monesin (20 μM) at 37°C. Cells were incubated at 37°C for the indicated times, the medium was drawn off and the cells were assayed for receptor-bound (precipitable) ^{125}I-ASOR using the procedure of Bridges et al. (6) as described in Materials and Methods. Data are the mean and standard errors of quadruplicate determinations. In this experiment the total cell-associated ^{125}I-ASOR, represented by parallel lines at one standard error above and below the mean, was 10 ng of ^{125}I-ASOR per 10^6 cells. The amount of ^{125}I-ASOR present in ligand-receptor complexes in control cells (diamonds) and in the presence of monensin (triangles) is shown after subtraction of background, defined as precipitable radioactivity in samples containing EDTA or in cells exposed to an excess of unlabeled ligand during the prebinding (<10% of the total in both cases). Ligand-receptor dissociation occurred rapidly in control cells; monensin completely blocked the dissociation.

endocytic vesicle acidification might be a general phenomenon that could play a role in the sorting of ligands and receptors after receptor-mediated endocytosis (20, 31, 32). In particular, since many ligands, including α_2-macroglobulin (20), low density lipoprotein (5), epidermal growth factor (13), lysosomal enzymes (12, 30), and asialoglycoproteins (6) are known to be dissociated from their receptors at pH 6.5 to 5.5, we proposed that endocytic vesicle acidification might drive ligand-receptor dissociation and allow unoccupied receptors to recycle from the endocytic vesicle back to the plasma membrane. We have shown that weak bases such as methylamine and monovalent ionophores such as monensin will cause a reversible dissipation of the endocytic vesicle pH gradient (20), and pharmacological studies measuring the effects of these agents on ligand and receptor distribution within the cell have provided indirect evidence in support of a role for endocytic compartment acidification in recycling of lysosomal enzyme (12), α_2-macroglobulin (33), and low density lipoprotein (4) receptors in fibroblasts, and for mannose receptors in macrophages (30).

Because of the likelihood that endocytic vesicle acidification is a requirement for receptor recycling in many cell types, we felt it was important to directly measure the pH of endocytic vesicles in another cell type and to couple these measurements with biochemical assays for ligand dissociation and receptor recycling. The asialoglycoprotein receptor was chosen for study because of the extensive characterization of endocytosis via this receptor (2, 3), and HepG2 cells were chosen because of the long lag time between internalization and degradation (Fig. 5; reference 26). Cells of the HepG2 human hepatoma line express about 250,000 asialoglycoprotein receptors per cell and the kinetics of endocytosis and degradation of ligand in these cells have been characterized (26). According to the model of Schwartz et al. (26), at half-saturating concentration of ligand a receptor binds a ligand, delivers it to the inside of the cell by endocytosis and recycles to the plasma membrane every 16 min. Since, under these same conditions, ^{125}I-ASOR is not degraded until ~45 min after internalization, this is a system in which receptor recycling is very clearly separated from ligand degradation (i.e., recycling appears to occur without involvement of lysosomes). We have not carried out a detailed kinetic analysis, but our measurements of the rate of return of unoccupied receptors to the cell surface (Fig. 9) and the dissociation of ligand from receptor (Fig. 13) seem to be in good agreement with the kinetic model of Schwartz et al. (26).

In the studies described here we used F-ASOR as a probe for the vesicle pH. We used cytochemical staining at the light and electron microscope level to confirm that pH measurements were made when ASOR is in structures that lack detectable acid-phosphatase activity. When cells were allowed to internalize F-ASOR at saturating concentrations for 10 min followed by rinsing and reincubation for 5 min, the spectroscopic characteristics of the specific F-ASOR fluorescence indicated a F-ASOR microenvironment pH of approximately 5.3–5.5. The vesicle pH was measured both by whole cell fluorescence intensity measurements and by image digitization. The combination of these two methods provides more information than either method alone: with the image digitization, we measure the pH of structures which appear as bright dots using image intensified fluorescence microscopy. Similar structures in fibroblasts have been shown to contain a mixture of several ligands that bind to cells through different

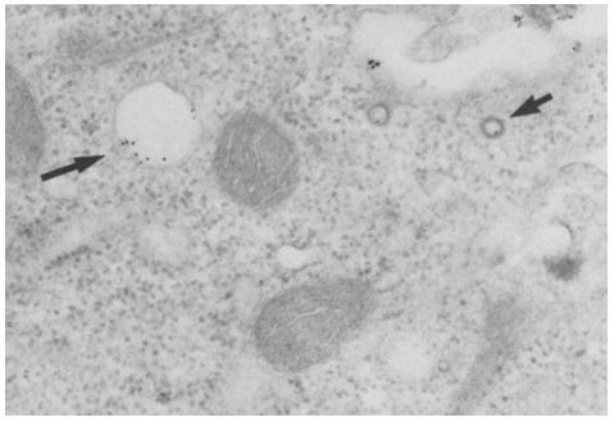

FIGURE 14 Monesin does not prevent transfer of prebound ligand to endocytic vesicles. HepG2 cells were incubated with ASOR-gold (5 μg/ml of adsorbed ASOR) in medium 1 at 4°C for 1 h. Cells were then rinsed with Dulbecco's modified Eagles's medium containing 2 mg/ml of bovine serum albumin and 10 μM monensin and reincubated for 10 min at 37°C. Cells were fixed in 2% glutaraldehyde and processed for electron microscopy. The gold particles were found in endocytic vesicles (long arrow) and occasionally in coated structures (short arrow) within the cell. No qualitative differences in the distribution of gold particles were observed when monensin-treated cells were compared with controls. Cisternae of the Golgi apparatus were dilated in monensin-treated cells (not shown); ASOR-gold was not found to be concentrated in the region of the Golgi apparatus in either control or monensin-treated cells. Bar, 1 μm.

receptors (19) and to undergo saltatory motion (23). Since it has been reported that ASOR is taken up by rat liver into a morphologically heterogeneous group of structures (35), it is possible that some portion of the F-ASOR is not in these bright dots. The observation that the same endocytic vesicle pH was obtained from whole cell intensity measurements indicates that all compartments that contain ASOR have approximately the same pH. We do not know what percentage of internalized F-ASOR is present in the dots such as those shown in Fig. 3. In trying to compare the pH of endocytic vesicles with the pH of lysosomes, we found that there was clearly a wide distribution of lysosome pH values. In this case, a whole cell intensity measurement would have yielded an "average" lysosomal pH which was much higher than the pH within most lysosomes.

In agreement with the predictions of a model in which receptor-ligand dissociation occurs in the acidified endocytic vesicle, we found that shifting the temperature from 37°C to 23°C inhibited ligand degradation by 90% while leaving the rate of receptor recycling unaffected. Endocytic vesicle acidification is essentially unimpaired at 23°C. Further support for this model was obtained from studies of the effects of agents which dissipate the vesicle pH gradient on the expression of asialoglycoprotein receptors at the cell surface. Both methylamine (35 mM) and monensin (20 μM) induced a rapid (within 10 min) ligand-independent loss of from 60 to 80% of the cell surface ^{125}I-ASOR binding capacity. The methylamine-induced loss was fully reversed within 1 h of rinsing in the presence of cycloheximide, suggesting that the lost receptors had been sequestered within the cell. Thus, agents that dissipate the endocytic vesicle pH gradient may interrupt continuous ligand-independent receptor recycling as has been suggested in other receptor systems (4, 12, 30). However, as is true of most experiments that use pharmacological inhibitors of cellular processes, these studies are open to more than one interpretation. For example, it is possible that dissipation of the endocytic vesicle pH gradient (or the pH gradients) causes depletion of receptors from the surface not by interrupting continuous recycling but rather by inducing internalization of receptors which would not normally move into the cell in the absence of ligand.

Since monensin dissipates the vesicle pH gradient within 2 min and does not prevent the internalization of prebound ligand, it was possible to directly test the hypothesis that vesicle acidification is necessary for ligand-receptor dissociation. Detergent solubilization of cells internalizing prebound ^{125}I-ASOR in the presence or absence of 20 μM monensin followed by precipitation of ligand-receptor complexes with ammonium sulfate showed that monensin completely blocks the separation of ligand from its receptor within the endocytic vesicle.

The results presented in this paper support a role for rapid endocytic vesicle acidification as the driving force for ligand-receptor dissociation in recycling systems. It must be emphasized that the studies reported here do not necessarily imply that receptors return to the plasma membrane directly from acidified primary endocytic vesicles. Re-acidifiction of endocytic vesicles upon removal of methylamine is complete within ~2 min, but the return of unoccupied receptors to the cell surface requires nearly 1 h for completion after removal of methylamine from the medium (Fig. 11). This is much longer than the normal recycling time for an internalized receptor (Fig. 9; reference 26). Monensin causes an essentially irreversible loss of receptors (Fig. 11). Ultrastructural localization (Fig. 14) shows that the occupied receptors in monensin treated cells enter tubulovesicular structures that are morphologically similar to the structures which contain receptors in untreated hepatocytes (9–11, 35). Re-acidification of these structures (Fig. 12) is not sufficient for recycling of receptors. The irreversibility of the monensin-induced loss of surface receptors suggests that the recycling pathway may traverse the Golgi apparatus or another organelle which is highly sensitive to monensin (27–29). In this connection, it has been reported that monensin induces trapping of low density lipoprotein receptors in a perinuclear region which was interpreted as Golgi apparatus (4). While direct evidence for involvement of the Golgi region in receptor recycling has not been reported, it has been shown that asialotransferrin is partially resialyated in the diacytotic pathway (25), suggesting that this ligand may in fact pass through the Golgi apparatus. Immunolocalization studies have been interpreted as demonstrating that the Golgi apparatus is not involved in ASG receptor recycling (10, 11). However, these conclusions are based on the steady state distribution of ASG receptors, and a rapid transit of receptors through the Golgi region would not be detected.

Taken in the context of previous studies of endocytic vesicle pH in mouse fibroblasts internalizing α_2-macroglobulin (31) and erythroleukemia cells internalizing transferrin (34), our results suggest that endocytic vesicle acidification is a general phenomenon common to many cell types. The promotion of receptor-ligand dissociation is only one of several possible "sorting" functions of the endocytic vesicle (32). For example, a strong case has been made for penetration of enveloped viruses into the cytoplasm from the acidified endocytic vesicle (18), and it has been suggested, based on studies of entry of prebound diphtheria toxin into the cytoplasm of cells exposed to low pH medium and on the protective effects of monovalent ionophores, that some bacterial toxins which have been shown to be internalized by receptor-mediated endocytosis (16) may gain access to the cytoplasm directly from endocytic vesicles (17). The full implications of endocytic vesicle acidification in directing the intracellular traffic of ligands and receptors remain to be defined by future work.

We are grateful to Dr. M. L. Shelanski and Dr. A. L. Schwartz for helpful advice. We wish to thank Sharon Fluss, Lois Bricken, Kristy Brown, Ann Francois, and Susan Hutchison for excellent technical assistance and Yvel Calderon and Julia Cohen for preparing the manuscript.

This work was supported by grants to F. R. Maxfield from the National Institutes of Health and the Irma T. Hirschl Charitable Trust and to M. L. Shelanski from the American Cancer Society.

Received for publication 18 March 1983, and in revised form 15 August 1983.

REFERENCES

1. Anderson, P., B. Tycko, F. Maxfield, and J. Vilcek. 1982. Effect of primary amines on interferon action. *Virology.* 117:510–515.
2. Ashwell, G., and J. Harford. 1982. Carbohydrate specific receptors of the liver. *Annu. Rev. Biochem.* 51:531–554.
3. Ashwell, G., and A. G. Morell. 1974. The role of surface carbohydrates in the hepatic recognition and transport of circulating glycoproteins. *Adv. Enzymol.* 41:99–128.
4. Basu, S. K., J. L. Goldstein, R. G. W. Anderson, and M. S. Brown. 1981. Monensin interrupts the recycling of low density lipoprotein receptors in human fibroblasts. *Cell.* 24:493–502.
5. Basu, S. K., J. L. Goldstein, and M. S. Brown. 1978. Characterization of the low density lipoprotein receptor in membranes prepared from human fibroblasts. *J. Biol. Chem.* 253:3852–3856.
6. Bridges, K., J. Harford, G. Ashwell, and R. D. Klausner. 1982. Fate of receptor and

ligand during endocytosis of asialoglycoproteins by isolated hepatocytes. *Proc. Natl. Acad. Sci. USA.* 79:350–354.
7. Cuatrecasas, P., and G. Illiano. 1971. Purification of neuraminidases from *Vibrio cholerae*, *Clostridium perfringens* and influenza virus by affinity chromatography. *Biochem. Biophys. Res. Commun.* 44:178–184.
8. Dickson, R. B., M. C. Willingham, and I. Pastan. 1981. α_2-Macroglobulin adsorbed to colloidal gold; a new probe in the study of receptor-mediated endocytosis. *J. Cell Biol.* 87:849–854.
9. Dunn, W. A., A. L. Hubbard, and N. N. Aronson, Jr. 1980. Low temperature selectively inhibits fusion between pinocytic vesicles and lysosomes during heterophagy of ^{125}I-asialofetuin by the perfused rat liver. *J. Biol. Chem.* 255:5971–5978.
10. Geuze, H. J., J. W. Slot, G. J. A. M. Strous, H. F. Lodish, and A. L. Schwartz. 1982. Immunocytochemical localization of the receptor for asialoglycoprotein in rat liver cells. *J. Cell Biol.* 92:865–870.
11. Geuze, H. J., J. W. Slot, G. J. A. M. Strous, H. F. Lodish, and A. L. Schwartz. 1983. Intracellular site of asiologlycoprotein receptor-ligand uncoupling: double-label immunoelectron microscopy during receptor-mediated endocytosis. *Cell.* 32:277–287.
12. Gonzalez-Noriega, A., J. H. Grubb, V. Talkad, and W. S. Sly. 1980. Chloroquine inhibits lysosomal enzyme pinocytosis and enhances lysosomal enzyme secretion by impairing receptor recycling. *J. Cell Biol.* 85:839–852.
13. Haigler, H. T., F. R. Maxfield, M. C. Willingham, and I. Pastan. 1980. Dansylcadaverine inhibits internalization of ^{125}I-epidermal growth factor in Balb 3T3 cells. *J. Biol. Chem.* 255:1239–1241.
14. Harford, J., A. Wolkoff, G. Ashwell, and R. D. Klausner. 1983. Intracellular dissociation of receptor-bound asialoglycoproteins in cultured hepatocytes. *J. Cell Biol.* 258:3191–3197.
15. Heiple, J. M., and D. L. Taylor. 1982. pH Changes in pinosomes and phagosomes in the ameba, *Chaos carolinensis*. *J. Cell Biol.* 94:143–149.
16. Keen, J. H., F. R. Maxfield, M. C. Hardegree, and W. H. Habig. 1982. Receptor-mediated endocytosis of diphtheria toxin by cells in culture. *Proc. Natl. Acad. Sci. USA.* 79:2912–2916.
17. Marnell, M. H., M. Stockey, and R. K. Draper. 1982. Monensin blocks the transport of diphtheria toxin to the cell cytoplasm. *J. Cell Biol.* 93:57–62.
18. Marsh, M., J. Wellsteed, H. Keru, E. Harms, and A. Helenius. 1982. Monensin inhibits Semliki Forest virus penetration into cultured cells. *Proc. Natl. Acad. Sci. USA.* 79:5297–5301.
19. Maxfield, F. R., J. Schlessinger, Y. Shechter, I. Pastan, and M. C. Willingham. 1978. Collection of insulin, EGF, and α_2-macroglobulin in the same patches on the surface of cultured fibroblasts and common internalization. *Cell.* 14:805–810.
20. Maxfield, F. R. 1982. Weak bases and ionophores rapidly and reversibly raise the pH of endocytic vesicles in cultured mouse fibroblasts. *J. Cell Biol.* 95:676–681.
21. Ohkuma, S., and B. Poole. 1978. Fluorescence probe measurement of the intralysosomal pH in living cells and the perturbation of pH by various agents. *Proc. Natl. Acad. Sci. USA.* 75:3327–3331.
22. Ohkuma, S., Y.Moriyama, and T. Takana. 1982. Identification and characterization of a proton pump on lysosomes by fluorescein isothiocyanate-dextran fluorescence. *Proc. Natl. Acad. Sci. USA.* 79:2758–2762.
23. Pastan, I. H., and M. C. Willingham. 1981. Journey to the center of the cell: role of the receptosome. *Science (Wash. DC).* 214:504–509.
24. Poole, B., and S. Ohkuma. 1981. Effect of weak bases on the intralysosomal pH in mouse peritoneal macrophages. *J. Cell Biol.* 90:665–669.
25. Regoeczi, E., P. A. Chindemi, M. T. Debanne, and P. A. Charlwood. 1982. Partial resialylation of human asialotransferrin type 3 in the rat. *Proc. Natl. Acad. Sci. USA.* 79:2226–2230.
26. Schwartz, A. L., S. E. Fridovich, and H. F. Lodish. 1982. Kinetics of internalization and recycling of the asialoglycoprotein receptor in a hepatoma cell line. *J. Biol. Chem.* 257:4230–4237.
27. Strous, G. J. A. M., and H. F. Lodish. 1980. Intracellular transport of secretory and membrane proteins in hepatoma cells infected by vesicular stomatitis virus. *Cell.* 22:709–717.
28. Tartakoff, A. M., and P. Vassalli. 1977. Plasma cell immunoglobulin secretion: arrest is accompanied by alterations of the Golgi complex. *J. Exp. Med.* 146:1332–1345.
29. Tartakoff, A. M. 1983. Perturbation of vesicular traffic with the carboxylic ionophore monensin. *Cell.* 32:1026–1028.
30. Tietze, C., P. Schlesinger, and P. Stahl. 1982. Mannose-specific endocytosis receptor of alveolar macrophages: demonstration of two functionally distinct intracellular pools of receptor and their roles in receptor recycling. *J. Cell Biol.* 92:417–424.
31. Tycko, B., and F. R. Maxfield. 1982. Rapid acidification of endocytic vesicles containing α_2-macroglobulin. *Cell.* 28:643–651.
32. Tycko, B., M. DiPaola, D. J. Yamashiro, S. Fluss, and F. R. Maxfield. 1983. Acidification of endocytic vesicles and intracellular pathways of ligands and receptors. *Ann. N.Y. Acad. Sci.* In press.
33. Van Leuven, F., J.-J. Cassiman, and H. Van Den Berghe. 1980. Primary amines inhibit recycling of α_2M receptors in fibroblasts. *Cell.* 20:37–43.
34. van Renswoude, J., K. R. Bridges, J. B. Harford, and R. D. Klausner. 1982. Receptor-mediated endocytosis of transferrin and uptake of Fe in K562 cells: identification of a nonlysosomal acidic compartment. *Proc. Natl. Acad. Sci. USA.* 79:6186–6190.
35. Wall, D. A., G. Wilson, and A. L. Hubbard. 1980. The galactose-specific recognition system of mammalian liver: the route of ligand internalization in rat hepatocytes. *Cell.* 21:79–93.
36. Warren, L. 1959. The thiobarbituric acid assay of sialic acids. *J. Biol. Chem.* 234:1971–1975.
37. Weigel, P. H., and J. A. Oka. 1982. Endocytosis and degradation mediated by asialoglycoprotein receptor in isolated rat hepatocytes. *J. Biol. Chem.* 257:1201–1207.